Journal of Applied Polymer Science

Crystallization behavior and polymorphism of poly(1,4-butylene adipate): Effect of anhydrous orotic acid as nucleating agent

Jinjun Yang,[1] Yichun Chen,[1] Lei Hua,[2] Rong Liang,[1] Dianxing Zhu[1]

[1]School of Environmental Science and Safety Engineering, Tianjin University of Technology, 391 Binshui Xidao, Xiqing District, Tianjin, 300384, China

[2]Department of Materials Science and Engineering, Zhejiang College of Tongji University, No. 168, Business Road, Jiaxing Zhejiang Province, 314051, China

J.Y. and Y.C. contributed equally to this work as co-first authors.

Correspondence to: J. Yang (E-mail: tjyjj_2014@tjut.edu.cn)

ABSTRACT: The effect of anhydrous orotic acid (OA), as a biocompatible nucleating agent (NA), on the non-isothermal and isothermal crystallization behaviors, polymorphic crystalline structure and phase transition of poly(1,4-butylene adipate) (PBA) was investigated. It is found that the OA increased the crystallization temperature of the PBA in the non-isothermal crystallization process and decreased the crystallization time of the PBA in the isothermal crystallization process. Meanwhile, the spherulite size decreased and spherulite density increased for the PBA. The OA favored the formation of the PBA α-form crystal, compared to the neat PBA. In addition, upon incorporation of the OA, the β-to-α phase transition rate was enhanced significantly. Mechanisms for the preferential formation of the PBA α-form crystal and the accelerated phase transition have also been proposed. © 2015 Wiley Periodicals, Inc. J. Appl. Polym. Sci. **2016**, *133*, 42957.

KEYWORDS: biodegradable; composites; crystallization; polyesters; properties and characterization

Received 31 July 2015; accepted 21 September 2015
DOI: 10.1002/app.42957

INTRODUCTION

Serious pollution to the environment, which has resulted from the use of traditional petroleum-based plastics without biodegradability, has attracted much attention from environmentalists, scientists, and engineers. Due to biodegradability, good processability, and mechanical properties, many efforts have been focused on the biodegradable polymers in scientific research and practical application. Generally, biodegradable polymers break down in physiological environments through hydrolytic macromolecular chain scission into smaller fragments, and ultimately into simple, stable end-products. The degradation may be due to aerobic or anaerobic microorganisms, biologically active processes (e.g., enzyme reactions) or passive hydrolytic cleavage.[1]

Aliphatic polyesters are important biodegradable and biocompatible polymeric materials which have been applied in agricultural, packaging, disposable products, and biomedical fields (such as tissue engineering, surgical sutures, gene therapy, controlled drug delivery), and their rapid development is in progress for the development of novel products with better performance.[2–7] Both poly(butylene adipate-*co*-terephthalate) (PBAT, Ecoflex®) and poly(butylene succinate-*co*-adipate) (PBSA, BIONOLLE®) are two kinds of representative polyester materials with biodegradability, and have been in mass production and widely applied in many fields. As a shared comonomer in both PBAT and PBSA, poly(1,4-butylene adipate) (PBA) is a typical linear aliphatic polyester that can be potentially used in eco-friendly and biomedical materials for its biodegradability.[1,8–11] Recently, much research has been focused on the PBA because of its peculiar relationship between polymorphic crystalline structure (aggregation structure), spherulite morphology, and biodegradation properties.[12–14]

Depending on the crystallization temperature (T_c), PBA can crystallize into the α-form crystal ($T_c \geq 32°C$), β-form crystal ($T_c \leq 28°C$), and (α+β) mixture ($29°C \leq T_c \leq 31°C$).[12] With respect to the lattice size of the crystal cell, the α-form, with a monoclinic cell unit, has a larger size than that of the β-crystal, with an orthorhombic cell. The crystallization rate of the β-form (the kinetically preferential phase) is higher than that of the α-form. At a lower heating rate (1°C/min) or a higher annealing temperature (T_a, 45°C) for a given length of time, the pure β-form gradually transforms into the α-crystal, suggesting that the α-form is the thermodynamically stable phase and the β-crystal metastable phase.[13] Both the α- and β-form crystal

show multiple melting peaks. The multiple melting behavior of the α-crystal is ascribed to a melt-recrystallization-remelt mechanism, and that of the β-form crystal is attributed to melt-phase transition-remelt mechanism.[13] Both the α- and β-form present the classic Maltese-cross ringless spherulite, but the $(\alpha+\beta)$ mixture exhibits the ring-band spherulite.[14] It is reported that the α-form with the larger crystal size and higher crystallinity shows a higher biodegradation rate than the β-one, which is inconsistent with expectation.[14] It is interesting that the $(\alpha+\beta)$ mixture with the ring banded spherulite shows the lowest biodegradation rate. Therefore, besides the crystal size and crystallinity, the biodegradability of the polymorphic polymeric material is also attributed to different packing characteristics of the polymer chain, including chain mobility, the surface structure of lamellar crystals, crystallization mechanisms, and chain interactions.[14] So, manipulation of polymorphic crystalline structure and control of spherulite morphology are effective approaches for tailoring of biodegradability of PBA.

Nucleating agents (NAs) are additives for the enhancement of the nucleus density and acceleration of crystallization rate. The NA has been used to tailor the microstructure and performance of the polymer. Therefore, addition of NAs is a widely accepted method in industrial technology and scientific research due to its low cost, convenience, and effectiveness. The incorporation of nucleating agents to the semi-crystalline polymers provides a surface on which the crystal growth can start. As a result, the enhanced crystallization rate will result in many small crystal domains. For example, the cycle times of polypropylene (PP) in injection molding decrease upon addition of NAs. In addition, the mechanical properties, such as heat distortion temperature, flexural modulus, strength and hardness increase, and the clarity and transmittance improve for PP after addition of NAs.[15,16]

To date, many NAs[17–27] have been used to increase the crystallization rate, and modulate the polymorphic crystalline structure and biodegradability of PBA, but the biocompatibilities of some NAs are still unclear, and preparation of other NAs is complicated. Orotic acid (OA) is an intermediate in the pyrimidine biosynthesis, which is required for DNA and RNA synthesis.[28] It was originally introduced as a vitamin, called vitamin B_{13}, but essentiality has not been demonstrated. OA occurs mainly in milk from ruminants, with highest amounts being found in animals which are deficient in arginine and uridine-5′-monophosphate activity. OA has also been detected in infant formula. Upon incorporation of the monohydrated OA, the crystallization rates of the polyhydroxybutyrate (PHB) and poly(hydroxybutyrate-*co*-hydroxyhexanoate) (PHBHHx) increase highly, and their crystallization time shorten significantly.[29,30] Tsui and Frank reported that compared to monohydrated OA, anhydrous OA was more effective as nucleating agent.[31] The faster crystallization of anhydrous OA leads to fibrillar morphology in the poly(hydroxybutyrate-*co*-hydroxyvalerate) (PHBV)/OA blends.[31] In addition, the substances possessing similar structure to OA, such as nucleobases[32] and cyanuric acid[33] were reported to significantly increase the crystallization rate and shorten the crystallization time of poly(L-lactide) and poly(3-hydroxylbutyrate) copolyester, respectively.

To date, the effect of OA on the crystallization kinetics, polymorphic crystalline structure of PBA has not been reported. In this work, anhydrous OA (for conciseness, anhydrous OA is abbreviated as OA) was selected as a biocompatible (benign), model NA to investigate its effects on the crystallization behavior, polymorphism, and phase transition of PBA. It is expected that small amount of OA (as nucleating agent) not only increases the crystallization rate and crystallization temperature but also adjusts polymorphic crystalline structure and phase transition.

EXPERIMENTAL

Materials

PBA ($M_w = 12000$ Da) was purchased from Sigma-Aldrich Co. Before use, PBA was purified by precipitating into ethanol from chloroform solution and then was dried under vacuum at 40°C for 1 week. OA was purchased from the Tokyo Chemical Industry (Japan), milled and dried at 60°C for 24 h under the vacuum before use.

Preparation of PBA/OA

The purified PBA was mixed with OA using a solution casting method to avoid the possible thermal degradation of the PBA in the melt-mixing. The detailed preparation processes are shown as follows. At first, OA with a given weight was dispersed uniformly in the chloroform (with ultrasonic treatment for an hour and the ratio of OA to chloroform is 0.1 g : 100 mL) as particles with sizes lower than 20 μm due to its insolubility. PBA (with a desired weight ratio to OA and the ratio of PBA to chloroform is 0.5 g : 100 mL) was then added into this suspension and stirred well. The chloroform was allowed to evaporate at room temperature. The resultant film was dried at 40°C under vacuum (about 50 Pa) for 24 h. In this work, the composite film sample is marked as PBA/x% OA, where x% is the weight percent of the OA.

Characterization

The thermal behavior of neat PBA and PBA/OA composites were measured using a Pyris Diamond differential scanning calorimetry (DSC) instrument (Perkin-Elmer, Waltham) equipped with a Perkin-Elmer intracooler 2P cooling accessory. The temperature and heat flow were calibrated using an indium standard under nitrogen purging. The sample (5–8 mg) was weighed and sealed in aluminum pans and melted at 100°C for 5 min to remove the thermal history. For the non-isothermal crystallization, the melted PBA was cooled to 0°C at a cooling rate of 10°C/min. For the isothermal crystallization, the melted PBA was cooled to the preset crystallization temperature (T_c) at a high cooling rate (100°C/min) and then held for a long enough time to complete the isothermal crystallization. After the non-isothermal and isothermal crystallization, the sample was reheated to 100°C at a rate of 10°C/min to investigate its subsequent melting behavior.

Polarized optical microscopy (POM) observation was performed on a XPF550C microscopy (Caikon Co., Shanghai, China) equipped with a digital camera. The sample was sandwiched between two glass slides, heated to 100°C at a rate of 10°C, and held for 5 min, followed by being pressed to form a thin and

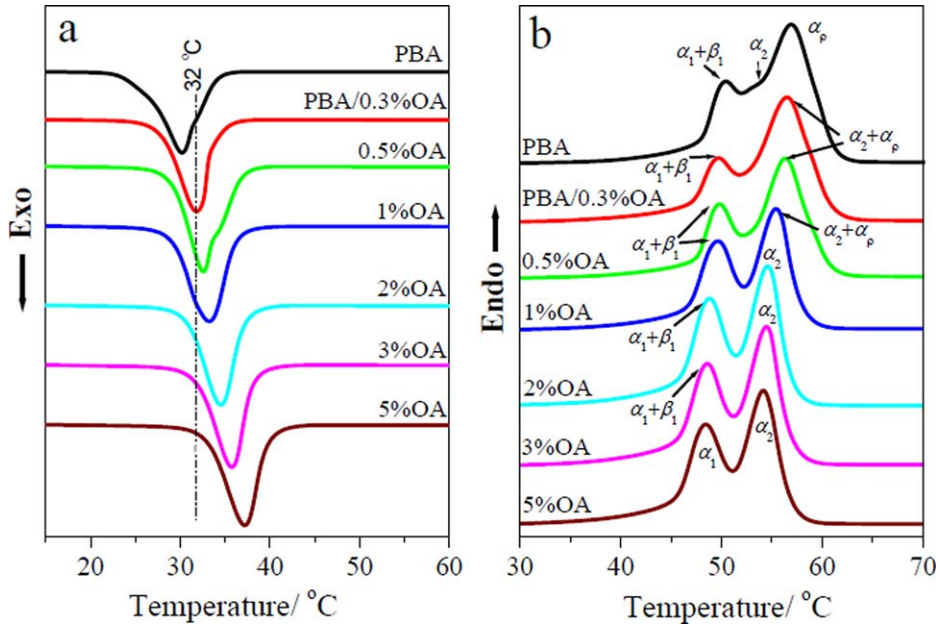

Figure 1. (a) Non-isothermal crystallization and (b) subsequent heating curves of neat PBA and OA-containing PBA. Both cooling rate and heating rate are 10°C/min. [Color figure can be viewed in the online issue, which is available at wileyonlinelibrary.com.]

melt layer of about 0.1 mm. Then the sample was rapidly transferred to a hot stage preset to desired temperatures for the isothermal crystallization. The spherulite morphology was recorded after completion of crystallization.

Wide-angle X-ray diffraction (WAXD) measurement was performed as follows. The sample was sandwiched between two iron plates with 1 mm thickness and pressed for 5 min at 100°C to form a thin and melt film of about 1 mm thickness on a hot press under 5 MPa, then was rapidly transferred on a hot stage (equipped with a liquid nitrogen cooling unit), preset to various T_cs for isothermal crystallization. For non-isothermal crystallization, the melt sample gradually crystallizes at a cooling rate of 10°C on this hot stage. After the completion of the isothermal and non-isothermal crystallization, the film sample was used for the WAXD measurement. For the PBA transition experiment, the pressed melt film sample was first placed on the hot stage preset at $T_c = 10$°C to obtain the pure PBA β-form crystal and then was transferred into the oven preset at annealing temperature (T_a) of 45°C for various lengths of time (30, 60, and 90 min). Finally, the sample was used for the WAXD measurement. All the WAXD patterns were recorded on a Rigaku RU-200 with Ni-filtered CuKα radiation ($\lambda = 0.154$ nm), worked at 40 kV and 200 mA (Rigaku Corp., Tokyo, Japan). The WAXD patterns were collected between Bragg angles of 5–40° at a scanning rate of 3°/min.

RESULTS AND DISCUSSION

Non-Isothermal Crystallization by DSC

Non-isothermal crystallization curves of neat PBA and OA-containing PBA are shown in Figure 1(a). It can be clearly seen that the crystallization temperature (T_c, the temperature at which the crystallization is fastest, as judged by the maximum in the exotherm of crystallization) of neat PBA is about 30°C and the crystallization peak is composed of two peaks which overlap at 32°C, denoted as the dash line. As aforementioned,[12,13] the PBA α-form and ($\alpha+\beta$) mixed crystal phase develop at $T_c \geq 32$°C and 29°C $\leq T_c \leq$ 31°C, respectively. From the non-isothermal crystallization curve of neat PBA, it can be speculated that the crystallization peak ranging from 25 to 35°C leads to the formation of the ($\alpha+\beta$) mixed crystal phase. With incorporation of OA, T_c of PBA increases gradually, suggesting that the OA plays a critical role in the nucleation of PBA at a low supercooling (that is, higher temperature). Additionally, upon increased loading (for example, 2, 3, and 5%) of OA, T_c of PBA shifts to 32°C, indicating that the developed PBA crystal is likely in the α-form. Therefore, the larger loading of OA appears to favor the formation of the PBA α-form.

The subsequent heating curves of neat PBA and OA-containing PBA are presented in Figure 1(b). Each heating curve shows two melting peaks. It is noteworthy that the melting temperatures of neat PBA is higher than those of OA-containing PBA. In addition, with an increase in the loading of OA, the melting temperatures slightly decrease. As aforementioned, addition of OA is favorable for the formation of PBA α-form. It was reported by Gan that the β-form has slightly higher melting temperatures, which is attributed to more energy used for the β-to-α transition in the heating process of β-form.[12,13] The multiple melting peaks of the α-form is ascribed to melt-recrystallization-remelt mechanism (a part of α-crystal would be melted, and the other part of α-crystal would recrystallize and become the α-crystal with more thickness or higher crystallinity) and that of the β-form to melt-phase transition-remelt mechanism (a part of β-crystal would be melted and the other part of β-crystal would transform into the α-crystal).[12,13] In the heating curve of 5% OA-containing PBA, the first melting peak maybe associated with the α_1-crystal (a part of originally formed

α-crystal) and the second one with the α_2-crystal (recrystallized α-crystal from the other part of originally formed α-crystal), because no β-form generates in this case (the crystallization temperature is higher than 32°C). When the loading of OA is from 0.3% to 3%, the first melting peak of the heating curve is probably the overlap of heating peaks (called as $\alpha_1+\beta_1$) result from the α_1-crystal and β_1-crystal (a part of original β-crystal), because the melting peak of the α_1 and β_1 crystal is very close. In cases of content of OA are 2% and 3%, the second melting peak is probably the α_2-crystal (no β-to-α phase transition occurs because the very small amount of β-form has been melt). In cases of content of OA are 0.3%, 0.5%, and 1%, the second melting peak is probably the overlap of the heating peaks of the α_2-crystal and α_p-crystal (the α-crystal transformed from the other part of β-crystal), that is, $\alpha_2+\alpha_p$. In the case of neat PBA, besides the melting peak assigned to $\alpha_1+\beta_1$, there are a shoulder peak (α_2) and α_p.

However, strictly speaking, the melting peaks in the DSC curve cannot be used for identification the polymorphism of PBA. The convincing evidence is available in the WAXD patterns, as shown in Figure 2. After the non-isothermal crystallization, the (α+β) mixed crystal (with the β-crystal as the predominant crystal type) develops, as judged by very strong diffraction peaks assigned to β (110) and β (020) and a very weak shoulder peak assigned to α (110). With an increase in the loading of OA (from 0.3% to 3%), the α (110) peak become more and more strong and the β (110) peak become more and more weak. Additionally, a new peak assigned to α (021) appears in cases of 2% OA and 3% OA. It can be concluded that the percentage of the α-crystal increases in the mixed phase. In the case of 5% OA, no diffraction peak assigned to the β-form can be seen, an indicative of the formation of the pure α-crystal. The WAXD result is consistent with the DSC result.

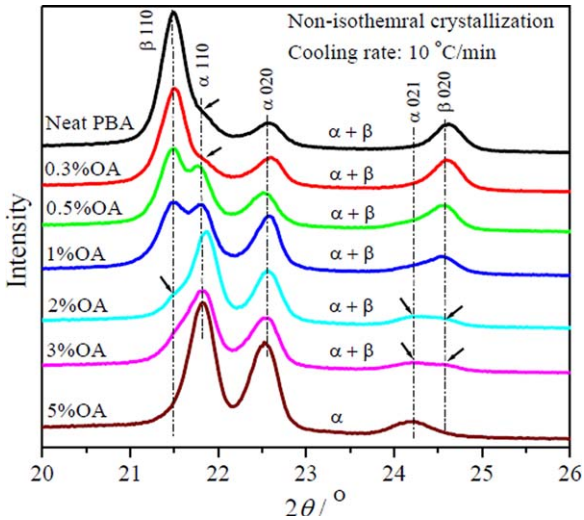

Figure 2. WAXD patterns of neat PBA and OA-containing PBA in the non-isothermal crystallization process at a cooling rate of 10°C. [Color figure can be viewed in the online issue, which is available at wileyonlinelibrary.com.]

Isothermal Crystallization by DSC

Due to the fast crystallization and high sensitivity to temperature for neat PBA, it is possible that a component of PBA has completed its crystallization before reaching the desired isothermal crystallization temperature (in particular below 30°C) from the fusion temperature (in this case, 100°C), even at a cooling rate of 100°C. It can be clearly seen that from the non-isothermal crystallization curves in Figure 1(a), a component of neat PBA has crystallized before reaching to 32°C. Furthermore, the addition of OA would increase the crystallization temperature of PBA, as shown in Figure 1(a). Here two higher crystallization temperatures (35 and 45°C) were selected as two examples to investigate the isothermal crystallization behavior, as presented in Figure 3. It can be clearly shown that with addition of OA and an increase in the loading of OA, the isothermal crystallization peak of the PBA sharpened and crystallization time shortened.

The Avrami equation is utilized to analyze quantitatively the isothermal crystallization kinetics and its linear form can be expressed as eq. (1).[34]

$$\log[-\ln(1-X_t)] = \log k + n\log t \quad (1)$$

where t is the crystallization time (min), X_t is the relative crystallinity at t (which can be calculated from the integrated area of the DSC curve from 0 to t divided by the integrated area of the whole heat flow curve), k is the crystallization rate constant, and n is the Avrami exponent related to both the nucleation mode (homogeneous or heterogeneous nucleation) and the dimension of the crystal growth. It is a combined function of the time dependence of nucleation (n_1) and the number of dimensions (n_2) in which crystal growth occurs, and can be expressed as $n = n_1 + n_2$.[35] For heterogeneous nucleation, $n_1 \approx 0$, which means that nuclei emerge all at once in the early stage of crystallization, that is, instantaneous nucleation. For homogeneous nucleation, $n_1 \approx 1$, and the number of nuclei increases with time. $n_2 = 1$, 2, and 3 represent 1-, 2-, and 3-dimensional growth, respectively. In practice, the obtained n values using the Avrami equation are not integers due to some uncertain factors.[10]

In Table I, the calculated isothermal crystallization kinetic parameters are shown. Upon incorporation of OA, the $t_{1/2}$ (crystallization half time) decreased and the k value for PBA increased, in the cases of $T_c = 35$ and 45°C. The n value of neat PBA is close to 4 regardless of the T_c, suggesting that the neat PBA spherulite grows in a homogeneous mode ($n_1 = 1$) in a 3-dimensional manner ($n_2 = 3$). After addition of OA, the n value is close to 3, indicating that the PBA spherulite still grows in a 3-dimensional manner ($n_2 = 3$) but in a heterogeneous mode ($n_1 = 0$).

Spherulite Morphology by POM

The spherulite morphologies of neat PBA and OA-containing PBA at various T_cs are shown in Figure 4. Neat PBA at $T_c = 30$°C, where the (α + β) mixture generates, shows the ring band spherulitic form (panel a_1). The spherulite size is increased and spherulite density is decreased at $T_c = 35$°C (panel a_2). With an increase in T_c to 40°C, the spherulite size is further increased and the spherulite density is further reduced (panel a_3), which is attributed to tendency to decreased nucleation under the smaller degree of supercooling.[AQ: Please check if

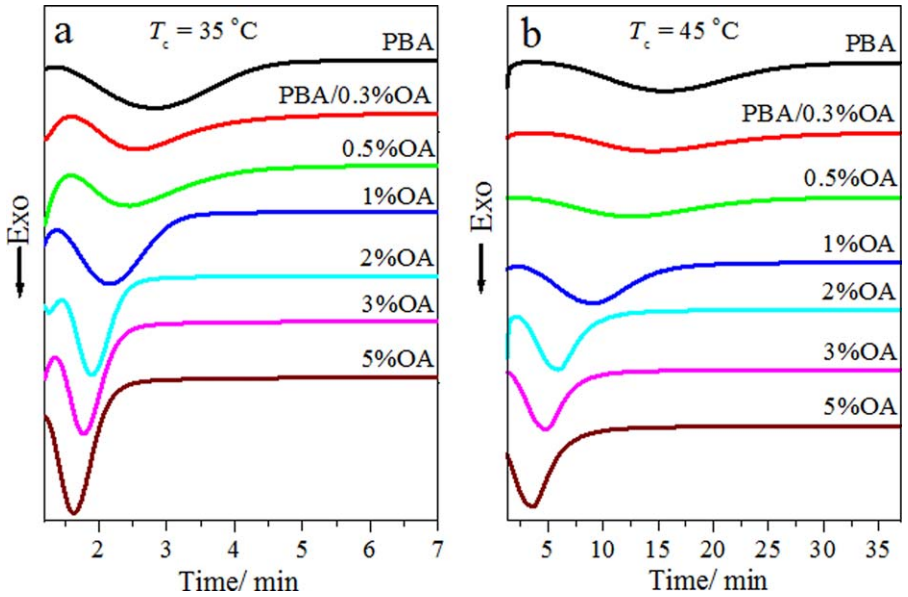

Figure 3. Isothermal crystallization curves of neat PBA and OA-containing PBA at T_c = (a) 35°C and (b) 45°C, respectively. [Color figure can be viewed in the online issue, which is available at wileyonlinelibrary.com.]

the edited sentence is OK as set and conveys the intended meaning.] After addition of 1% (panels b_1, b_2, and b_3) and 3% (panels c_1, c_2, and c_3) OA, the spherulite size decreased and spherulite density increased significantly at the same T_c, compared with the neat PBA. It can be concluded from the POM observations that OA has effective nucleation ability on the

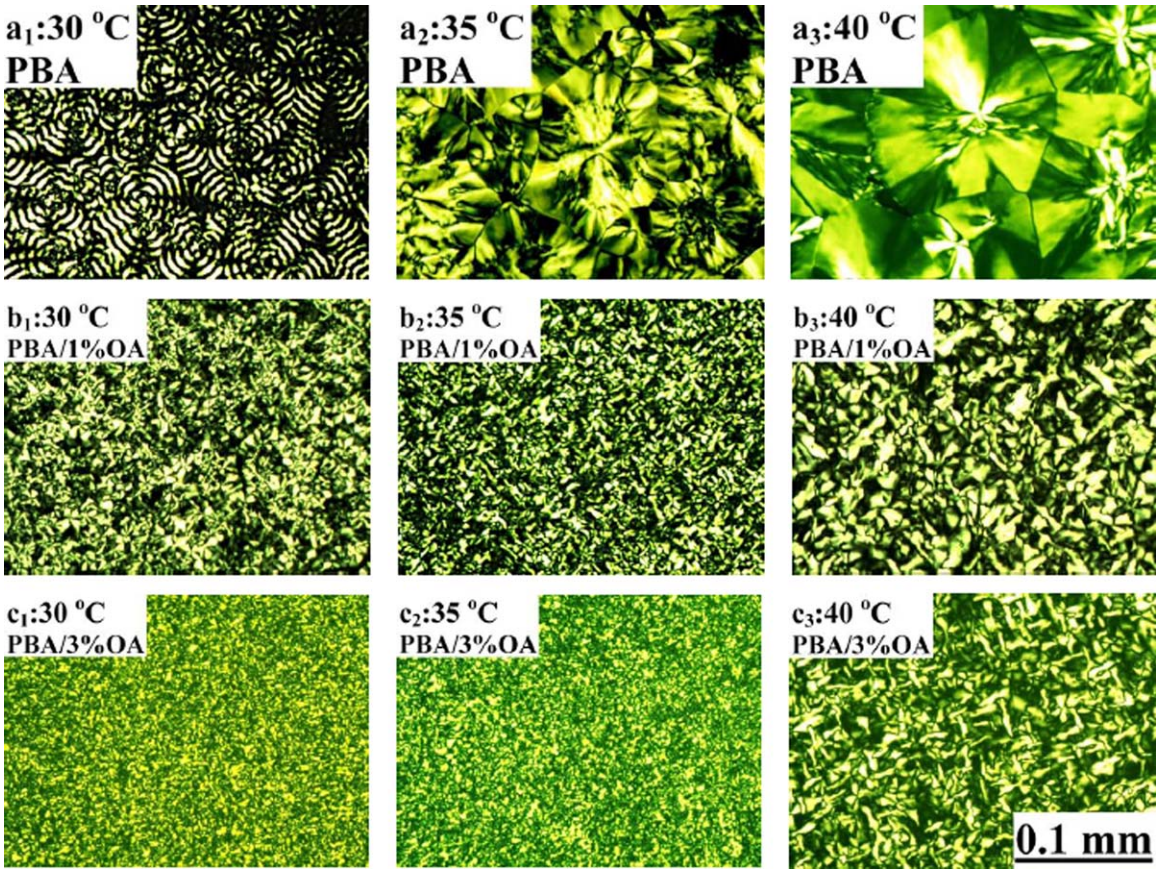

Figure 4. Spherulite morphologies of neat PBA and OA-containing (1% and 3% loading of OA) PBA at various T_cs. [Color figure can be viewed in the online issue, which is available at wileyonlinelibrary.com.]

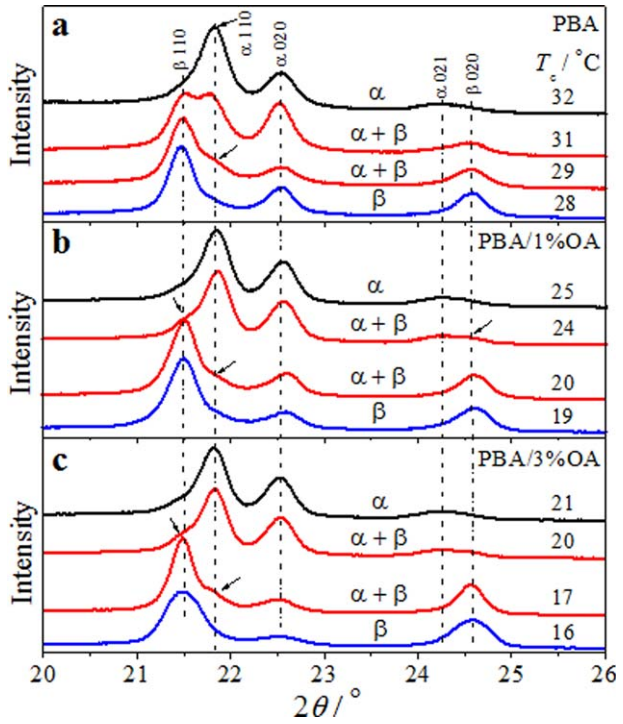

Figure 5. The WAXD patterns of PBA melt-crystallized at various T_cs upon loading of (a) 0% OA (neat PBA), (b) 1% OA, and (c) 3% OA. [Color figure can be viewed in the online issue, which is available at wileyonlinelibrary.com.]

crystallization of the PBA, and that OA can serve as heterogeneous nuclei and decrease the free energy for the formation of a critical nucleus for PBA.

Polymorphic Crystalline Structure by WAXD

The α- and β-crystal forms of PBA have their own characteristic diffraction peaks in the WAXD pattern, which locate at different 2θ angles. The β-form exhibits two characteristic diffraction peaks, assigned to β (110) and β (020), respectively; and the α-form shows three characteristic diffraction peaks, assigned to α (110), α (020), and α (021), respectively, as shown in Figure 5(a). At $T_c \leq 28$°C, the pure β-form of PBA developed, in line with expectation; at $T_c \geq 32$°C, pure α-form crystallized (for brevity, the lowest T_c where pure α-form develops is called $T_{c,\alpha}$); at $29°C \leq T_c \leq 31°C$, the $(\alpha + \beta)$ crystal mixture developed, that is, the β- and α-forms coexisted (and the lowest T_c at which the α-form of PBA emerges is called $T_{c,e}$). There is good agreement with the previous results.[12,13] Upon loading of 1% OA, both the $T_{c,e}$ and $T_{c,\alpha}$ of PBA decreased to 20 and 24°C, respectively [Figure 5(b)]. With a further increase in the loading of OA, the $T_{c,e}$ and $T_{c,\alpha}$ decreased to 17 and 20°C, respectively [Figure 5(c)]. It suggests that the addition of the OA facilitated the formation of the PBA α-crystal.

To describe directly the effect of OA on PBA polymorphism, the T_c values (as examined by the WAXD measurement) of the PBA α- and β-forms are plotted as a function of the loading of OA, as presented in Figure 6. From this figure, it can be seen that the $T_{c,e}$ and $T_{c,\alpha}$ of the PBA decreased monotonously with an increase in the loading of OA. Proposed mechanism for preferential formation of the PBA α-form will be given later.

Phase Transition Annealing at 45°C by WAXD

To investigate further effect of OA on the phase transition of PBA, the WAXD measurement of PBA at different loadings of OA after annealing for various lengths of time has been performed. Here, 10°C is chosen as the recrystallization temperature for developing the pure PBA β-form and 45°C (lower than the melting temperature of PBA) is selected as the annealing temperature.

Only a weak diffraction peak assigned to α (110) can be found even at $t_a = 90$ min at 45°C (as shown in Figure 7(a)), suggesting that very little of the PBA β-form has transformed into the α-form and the phase transition is slow for the neat PBA. Upon addition of 1% OA [Figure 7(b)], the diffraction peak assigned to α (110) at $t_a = 90$ min shows a higher intensity than that in Figure 7(a), an indicator of accelerated phase transition. With further increase in the loading of OA to 3% [Figure 7(c)], the α (110) diffraction peak became a separate one at $t_a = 60$ and 90 min, revealing that the phase transition is accelerated significantly, compared to neat PBA. In the case of 5% OA, the diffraction peaks assigned to β (110) and β (020) had disappeared by $t_a = 90$ min (data not shown), suggesting that β-form has transformed into α-form completely. The rearrangement or adjustment of the PBA molecular chain accounts for the β-to-α phase transition. Based on the differences in the crystal lattice structure between β- and α-form, three kinds of molecular chain motion in lattice cell, such as bond shift, rotation, and shrink, are proposed for enabling the phase transition process of PBA.[13]

Plausible Mechanism for Preferential formation of PBA α-form Crystal and Accelerated Phase Transition under OA Nucleation

Based on the classical metastable theory,[36,37] the metastable phases are considered to fall into one of the multiple local free energy minima in the Gibbs free energy profiles and will ultimately transform into the thermodynamically stable state of minimum global free energy. Among the crystal forms, all but

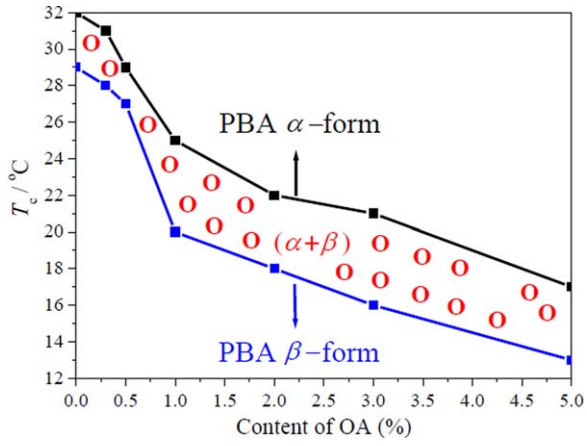

Figure 6. Content of OA-dependent T_c of the PBA α- and β-form in the PBA/OA composite. [Color figure can be viewed in the online issue, which is available at wileyonlinelibrary.com.]

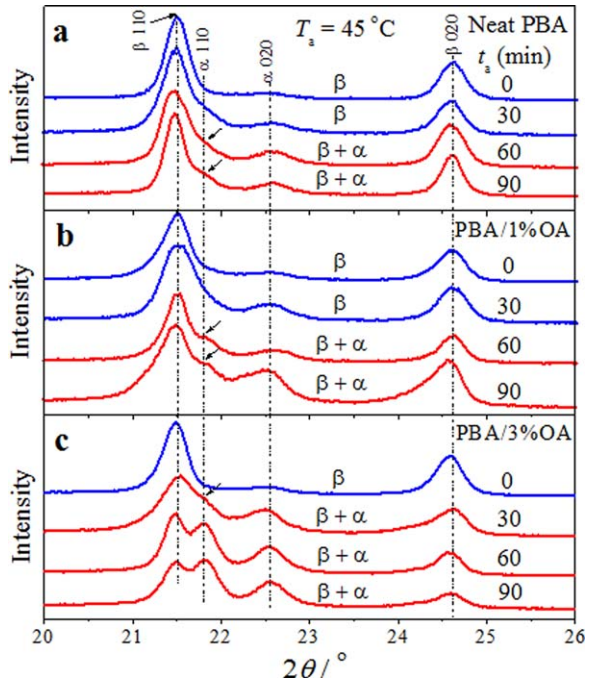

Figure 7. WAXD patterns of the PBA component in the PBA/OA annealing at 45°C for various time lengths with OA loading of (a) 0%, (b) 1%, and (c) 3%. [Color figure can be viewed in the online issue, which is available at wileyonlinelibrary.com.]

one is in a metastable state at a specific temperature and pressure. In this case, as a metastable phase, the formation of the PBA β-form is usually due to the kinetic effects which provide a favorable pathway for the polymer to fall into the local free energy minimum.[13] In this case, the nucleation in crystallization was increased due to the interface between PBA and OA, which is ascribed to a decrease in the surface free energy of formation of crystal nuclei in the presence of the phase interface.[38–42] The depression in the surface energy accelerated the nucleation and improved the mobility of the polymer chain near the interface,[43] leading to the decrease of T_c of the α-form.

From the thermodynamics viewpoint, the depression of T_c (especially in the miscible blending pair) of the polymer is probably ascribed to the reduction of its equilibrium melting point (T_m^0). The Hoffman-Weeks method was used to examine the $T_m{}^0$ of the PBA α-form crystal by drawing a plot of T_c vs T_m.[44] Here, the T_c is the isothermal crystallization temperature (such as 35, 38, 40, 42, and 45°C) of the pure α-form crystal and T_m is the first melting temperature in the subsequent heating process. It is found that after addition of OA, the T_m of PBA pure α-form crystal is nearly unaltered, suggesting that it is T_m^0 changed little (data not shown). Thus, the thermodynamic effect can be excluded as an explanation for the preferential formation of the α-form in this work.

It is necessary to obtain enough energy to overcome the energy barrier to realize the phase transition. It was observed that thickening of the PBA lamellae occurred after annealing at 40°C for 1 h, but no β-to-α transition could be observed because the obtained energy at 40°C is lower than the critical energy barrier.[13] As aforementioned, the $T_{c,e}$ and $T_{c,\alpha}$ of PBA decreased after addition of OA. Accordingly, the critical energy barrier for the PBA phase transition must have also reduces. Thus at the same annealing temperature (in this case, $T_a = 45$°C), because of the greater temperature difference of ($T_a - T_{c,e}$) in the presence of the OA, it can provide more energy to accelerate the phase transition of the PBA, compared to the neat PBA. That is, the obtained energy during the annealing is the predominant driving force for the phase transition.

CONCLUSIONS

The OA increased the crystallization temperature of the PBA, attributed to the fact that the OA plays a critical role on the nucleation of the PBA at a low supercooling. After addition of the OA, crystallization rate increased and the crystallization time shortened for the PBA. POM result suggested that in the composite, the spherulite size is smaller and spherulite density is larger than that of neat PBA, revealing that the OA has an effective nucleating ability as a heterogeneous nucleating agent. Upon incorporation of the OA, the $T_{c,e}$ and T_a reduced. It is probably ascribed to decreasing of the surface free energy of nucleus upon incorporation of OA and the kinetically preferential growth of the PBA β-form, resulting in the shift of the $T_{c,e}$ and $T_{c,\alpha}$ of the PBA to lower temperature region. In the presence of the OA, the phase transition rate of the PBA increased. It should be attributed to the greater temperature difference of ($T_a - T_{c,e}$) in the presence of the OA, it can provide more energy to accelerate the phase transition of the PBA, compared to the neat PBA. That is, OA not only facilitated the formation of the PBA α-form crystal and modified the polymorphic

Table I. Kinetic Parameters of PBA in the Isothermal Crystallization (35 and 45°C) Process for Neat PBA and OA-Containing PBA

	T_c = 35°C			T_c = 45°C		
Sample	$t_{1/2}$ (min)	n	k (min^{-1})	$t_{1/2}$ (min)	n	k (min^{-1})
PBA	2.61	4.2	5.1	18.03	4.1	8.9×10^{-7}
PBA/0.3% OA	2.48	3.1	6.3	17.39	3.1	4.3×10^{-6}
PBA/0.5% OA	2.39	2.9	7.2	16.11	3.0	1.6×10^{-6}
PBA/1% OA	1.99	3.0	9.1	13.27	3.2	8.2×10^{-5}
PBA/2% OA	1.62	2.8	10.2	10.28	2.9	3.1×10^{-5}
PBA/3% OA	1.58	2.8	12.4	8.53	2.9	1.9×10^{-4}
PBA/5% OA	1.49	2.9	14.8	7.14	2.7	6.8×10^{-3}

crystalline structure of PBA, but also accelerated significantly the β-to-α transition of PBA. It is easy to modulate the polymorphic crystalline structure and phase transition of the PBA via addition of the OA.

ACKNOWLEDGMENTS

This work was financially supported by the "National Natural Science Foundation of China (No. 21304070)", "Program of Study Abroad for Young Scholar sponsored by Tianjin Municipal Education Commission (the ninth batch), China" and "Training Programs of Innovation and Entrepreneurship for Undergraduates in Colleges and Universities of Tianjin, China (No. X2014015)".

REFERENCES

1. Pan, P.; Inoue, Y. *Prog. Polym. Sci.* **2009**, *34*, 605.
2. Nair, L. S.; Laurencin, C. T. *Prog. Polym. Sci.* **2007**, *32*, 762.
3. Doi, Y.; Steinbüchel, A. Biopolymers. Polyester III. Applications and Commercial Products; Wiley-VCH: Weinheim, **2002**.
4. Im, S. S.; Kim, Y. H.; Yoon, J. S.; Chin, I. J. Bio-Based Polymers: Recent Progress; Wiley-VCH: Weinheim, **2005**.
5. Ikada, Y.; Tsuji, H. *Macromol. Rapid Commun.* **2000**, *21*, 117.
6. Misra, S. K.; Valappil, S. P.; Roy, I.; Boccaccini, A. R. *Biomacromolecules* **2006**, *7*, 2249.
7. Iwata, T.; Doi, Y. *Macromol. Chem. Phys.* **1999**, *200*, 2429.
8. Yang, J.; Pan, P.; Hua, L.; Feng, X.; Yue, J.; Ge, Y.; Inoue, Y. *J. Phys. Chem. B* **2012**, *116*, 1266.
9. Yang, J.; Pan, P.; Hua, L.; Xie, Y.; Dong, T.; Zhu, B.; Inoue, Y.; Feng, X. *Polymer* **2011**, *52*, 3460.
10. Yang, J.; Pan, P.; Hua, L.; Zhu, B.; Dong, T.; Inoue, Y. *Macromolecules* **2010**, *43*, 8610.
11. Yang, J.; Li, Z.; Pan, P.; Zhu, B.; Dong, T.; Inoue, Y. *J. Polym. Sci. Polym. Phys.* **2009**, *47*, 1997.
12. Gan, Z.; Abe, H.; Doi, Y. *Macromol. Chem. Phys.* **2002**, *203*, 2369.
13. Gan, Z.; Kuwabara, K.; Abe, H.; Iwata, T.; Doi, Y. *Biomacromolecules* **2004**, *5*, 371.
14. Gan, Z.; Kuwabara, K.; Abe, H.; Iwata, T.; Doi, Y. *Polym. Degrad. Stab.* **2005**, *87*, 191.
15. Horváth, Z.; Menyhárd, A.; Doshev, P.; Gahleitner, M.; Vörös, G.; Varga, J.; Pukánszky, B. *ACS Appl. Mater. Interfaces* **2014**, *6*, 7456.
16. Gahleitner, M.; Grein, C.; Kheirandish, S.; Wolfschwenger, J. *Int. Polym. Proc.* **2011**, *26*, 2.
17. Jiang, N.; Zhao, L.; Gan, Z. *Polym. Degrad. Stab.* **2010**, *95*, 1045.
18. Dong, T.; Kai, W.; Inoue, Y. *Macromolecules* **2007**, *40*, 8285.
19. Kai, W.; Zhu, B.; He, Y.; Inoue, Y. *J. Polym. Sci. Polym. Phys.* **2005**, *43*, 2340.
20. Zhao, Y.; Qiu, Z. *CrystEngComm* **2011**, *13*, 7129.
21. Tang, Y.; Xu, J.; Guo, B. *Ind. Eng. Chem. Res.* **2015**, *54*, 1832.
22. Huang, S.; Qiu, Z. *Ind. Eng. Chem. Res.* **2014**, *53*, 15296.
23. Weng, M.; He, Y.; Qiu, Z. *Ind. Eng. Chem. Res.* **2012**, *51*, 13862.
24. Zhao, Y.; Qiu, Z. *J. Nanosci. Nanotechnol.* **2012**, *12*, 4067.
25. Wang, G.; Qiu, Z. *Ind. Eng. Chem. Res.* **2014**, *53*, 1712.
26. Chen, Y.; Wu, T. M. *Ind. Eng. Chem. Res.* **2014**, *53*, 16689.
27. Yang, J.; Chen, Y.; Qin, S.; Liu, J.; Bi, C.; Liang, R.; Dong, T.; Feng, X. *Ind. Eng. Chem. Res.* **2015**, *54*, 8048.
28. Bhattacharjeea, S.; Bhattacharya, S. *Chem. Commun.* **2015**, *51*, 6765.
29. Jacquel, N.; Tajima, K.; Nakamura, N.; Miyagawa, T.; Pan, P.; Inoue, Y. *J. Appl. Poly. Sci.* **2009**, *114*, 1287.
30. Jacquel, N.; Tajima, K.; Nakamura; Kawachi, H.; Pan, P; Inoue, Y. *J. Appl. Poly. Sci.* **2010**, *115*, 709.
31. Tsui, A.; Frank, C. W. *Polymer* **2014**, *55*, 6364.
32. Pan, P.; Yang, J.; Shan, G.; Bao, Y.; Wang, Z.; Inoue, Y. *Macromol. Mater. Eng.* **2012**, *297*, 670.
33. Pan, P.; Shan, G.; Bao, Y.; Wang, Z. *J. Appl. Polym. Sci.* **2013**, *129*, 1374.
34. Gedde, U. W. Polymer Physics; Chapman & Hall: London, **1995**.
35. Pan, P.; Liang, Z.; Nakamura, N.; Miyagawa, T.; Inoue, Y. *Macromol. Biosci.* **2009**, *9*, 585.
36. Keller, A.; Cheng, S. Z. D. *Polymer* **1998**, *39*, 4461.
37. Pan, P.; Liang, Z.; Zhu, B.; Dong, T.; Inoue, Y. *Macromolecules* **2009**, *42*, 3374.
38. Liang, Z.; Yang, J.; Hua, L.; Pan, P.; Huang, J.; Zhang, J.; Abe, H.; Inoue, Y. *J. Appl. Poly. Sci.* **2014**, *131*, 39600.
39. Bartczak, Z.; Galeski, A.; Krasnikova, N. P. *Polymer* **1987**, *28*, 1627.
40. Wenig, W.; Asresahegn, M. *Polym. Eng. Sci.* **1993**, *33*, 877.
41. Tsuburaya, M.; Saito, H. *Polymer* **2004**, *45*, 1027.
42. Zhang, X. H.; Wang, Z. G.; Muthukumar, M.; Han, C. C. *Macromol. Rapid Commun.* **2005**, *26*, 1285.
43. Sakai, F.; Nishikawa, K.; Inoue, Y.; Yazawa, K. *Macromolecules* **2009**, *42*, 8335.
44. Hoffman, J. D.; Weeks, J. *J. Res. Natl. Bur. Stand.* **1962**, *66A*, 13.